Journal of Materials Chemistry B

Accepted Manuscript

ROYAL SOCIETY OF CHEMISTRY

www.rsc.org/materialsB

Journal Name

RSCPublishing

ARTICLE

Synthesis and characterization of water soluble biomimetic chitosans for bone and cartilage tissue regeneration

Cite this: DOI: 10.1039/xoxxoooooox

Received ooth January 2012,
Accepted ooth January 2012

DOI: 10.1039/xoxxoooooox

www.rsc.org/

Megan S. Lord,*[a] Bonny M. Tsoi,[a] Brooke L. Farrugia,[a] S. R. Simon Ting,[a, #] Shenda Baker,[b] William P. Wiesmann,[b] John M. Whitelock[a]

Chitosan, a polysaccharide derived from the exoskeleton of crustaceans, insects, the cell walls of fungi, the radulas of molluscs and the internal shells of cephalopods and has been shown to promote osteogenesis. Arginine functionalized chitosan, a water soluble derivative of chitosan, was successfully sulfated with a degree of sulfur incorporation of up to 9% with substitution at the 2-N position. This degree of sulfation replicated those of naturally occurring growth factor binding glycosaminoglycans. Sulfated chitosan-arginine was found to bind and signal fibroblast growth factor 2. Chitosan-arginine promoted an osteogenic phenotype in primary human fetal chondroblasts over a period of 7 days in the absence of osteogenic medium while sulfated chitosan-arginine promoted a chondrogenic phenotype in these same cells. Together these data demonstrate that fine control over progenitor cell phenotype can be achieved in the presence of sulfate modified chitosan-arginine that promotes further investigation and potential development in the future for applications requiring osteo-chondral repair.

Introduction

Chitosan, a deacetylated derivative of chitin, is a naturally occurring polysaccharide composed of β-(1→4)-linked GlcN and GlcNAc units. In an acidic environment, chitosan exhibits anti-microbial, anti-inflammatory and wound healing properties[1,2] while this material is also not cytotoxic[3-7] Chitosan is often derivatized or copolymerized to enhance its biological properties. As chitosan is soluble in acetic acid, its natural insolubility at physiologic pH limits its use in clinical applications. However, chitosan is made to be soluble in water by modification with the amino acid, arginine,[8] through functionalization to form stable bonds between the carboxylic acid on arginine and the amine on the glucosamine residues of chitosan. Chitosan-poly(arginine), which has multiple arginine moieties from a single amine on the backbone, has been explored for the efficient gene transfection of cells,[9-11] as an anti-coagulant,[12] as an anti-microbial[8, 13] and as an enhancer of transdermal drug delivery.[14] The arginine functionalization of chitosan provides an overall positive charge that enhances cell surface binding and uptake.[10] The chitosan-arginine used in this study is functionalized with arginine through a controlled reaction to yield a single arginine per amine on the chitosan backbone.[15]

Sulfated forms of chitosan have gained some research focus for their ability to mimic naturally occurring sulfated biopolymers, such as heparin and chondroitin sulfate, which have important functions in the regulation of cellular proliferation and differentiation.[16] These sulfated biopolymers are found naturally as the glycosaminoglycan chains of proteoglycans. Sulfated forms of chitosan have been explored as synthetic analogues of the anti-coagulant, heparin,[12, 17] as well as growth factor binding activities of heparan sulfate.[18]

Proteoglycans are a major component of the cartilage extracellular matrix with important roles in stimulating both chondrogenesis and osteogenesis through interactions with collagens and growth factors.[19, 20] These interactions are dependent on the structure of the glycosaminoglycans, heparan and chondroitin sulfate.[21, 22] GAG-augmented chitosan hydrogels have been shown to promote a chondrogenic phenotype in bovine primary articular chondrocytes.[23] In contrast, chitosan-poly(arginine) exposed to myoblastic precursor cells with osteoblastic potential, C2C12 cell line, together with bone morphogenic protein (BMP)-2 promote the osteoblast phenotype of these cells.[24, 25] Additionally, sulfated chitosan coated BMP-2 loaded calcium-deficient hydroxyapatite scaffolds have been reported to promote bone formation in a rat full-thickness bone defect model.[26] However, the effects of chitosan and sulfated chitosan alone on cell phenotype remain to be investigated.

Therefore, the aims of this study were to sulfate chitosan-arginine for the first time, determine its ability to bind and signal growth factors as well as to promote either an osteoblastic or chondrogenic phenotype using primary human fetal chondro-progenitor cells. This study has shown that human progenitor cells in contact with water soluble chitosan-arginine alone can promote bone formation while when these same cells are placed in contact with sulfated chitosan-argnine form cartilage.

Experimental

Materials

Chitosan-arginine (CH-Arg) (85% deacetylated with arginine constituting 24% of the total monomers on the polymer backbone; 57 kDa, purity > 99%) was synthesized by Synedgen, Inc. Porcine sub-intestinal mucosal heparin (180 IU/mg, molecular mass 18,000 Da was sourced from Sigma Aldrich (Castle Hill, NSW, Australia). Human fetal knee joints (12-14 week old) were harvested in accordance with institutional approval from the Human Research Ethics Committee of The University of New South Wales. The monoclonal mouse anti-collagen type I (clone I-8H5) and monoclonal mouse anti-collagen type II (clone II-4C11) antibodies were purchased from ICN Biomedicals (Seven Hills, Australia). The monoclonal mouse anti-human aggrecan (clone 969D4D11) was purchased from Life Technologies (Sydney, Australia). The polyclonal rabbit anti-human perlecan (CCN-1) was raised in house against immunopurified human coronary artery endothelial cell perlecan.[27] All other chemicals were purchased from Sigma Aldrich (Castle Hill, Australia) unless stated otherwise.

Sulfation of CH-Arg

Homogeneous sulfation of CH-Arg

30 mL DMF was cooled to 0 – 4 ^{o}C in an ice bath. DMF was removed from the ice bath, placed at room temperature (RT) and 5 mL of $HClSO_3$ was added dropwise to the DMF while stirring with a magnetic stirrer. Stirring continued until the resultant DMF·SO_3 reached RT. 1 g of CH-Arg was dissolved in 20 mL formic acid within 3 h at RT. 156 mL of DMF is added, and the mixture was stirred for 2 h using a magnetic stirrer. DMF·SO_3 was dropped slowly into the solution in either an excess or enough to sulfate half of the available modification sites on the chitosan backbone within 30 min and the mixture was kept at 55 ^{o}C for 1 - 3 h. The solution was then left to cool to RT, and the product was poured into 600 mL saturated alkaline ethanolic solution of anhydrous sodium acetate. The precipitate that formed was washed with a mixture of ethanol and DI water (ethanol:DI water, 4:1, v:v) and subsequently dissolved in DI water. The pH of the solution is adjusted to 7.5. The resultant solution was dialyzed against deionized water for 48 h using a 10 kDa dialysis cut-off membrane and lyophilized.

2-N sulfation of CH-Arg

Lyophilized CH-Arg (1g) was dispersed in 75 mL of DI water under gentle agitation. 2 g of 15 mmol Na_2CO_3 was added to maintain an alkaline environment (pH > 9) and 3 g of 25 mmol sulfur trioxide pyridine complex (Me_3N-SO_3) complex was added to the solution to start the reaction. The mixture was heated and the reaction was maintained at 60 ^{o}C for 12 h under an argon atmosphere. A few drops of 1M HCl were added to the mixture to achieve a neutral pH. After being cooled to RT, the mixture was dialyzed in succession against deionized water, 4 L of aqueous solution of 0.025 M NaOH and finally against DI water for 24 h per stage, using a 10 kDa dialysis cut-off membrane and lyophilized.

Characterization of sulfated CH-Arg

A Perkin Elmer Spotlight 400 Attenuated total reflectance-fourier transform infra-red spectroscopy (ATR-FTIR) was used to measure changes in the surface chemical structure of the CH-Arg following sulfation. Spectra were recorded between 650 and 4000 cm^{-1}. X-ray photoelectron spectroscopy (XPS) spectra were obtained for CH-Arg and the sulfated derivatives using a Thermo ESCALAB250i X-ray Photoelectron Spectrometer (XPS) with elemental mapping capability and He UV Source (UPS). The degree of sulfation was calculated according to the contents of sulfur (S%) and nitrogen (N%) in the sample using the formula, DS= (S%/32.06)/(N%/14.007). The 2D-NMR as HSQC (^{1}H detected heteronuclear single quantum coherence) were conducted on a Bruker Avance III 300 NMR operating at 20 °C with a frequency of 600 MHz and an acquisition time of up to 5.5 s. The samples were dissolved in D_2O and 16 to 32 scans were acquired.

Growth factor binding and signaling activity of sulfated CH-Arg

BaF32 cells are from an IL-3-dependent and heparan sulfate proteoglycan deficient myeloid B cell line that has been stably transfected with fibroblast growth factor receptor (FGFR) 1c.[28, 29] BaF32 cells represent a model system developed to identify heparin/ heparan sulfate structures that interact with FGFs and their receptors. The readout of this assay is cell proliferation which indicated the formation of ternary complexes on the cell surface between heparin/ heparan sulfate, FGF-2 and FGFR1c.[28] BaF32 cells were maintained in RPMI 1640 medium containing 10% (v/v) fetal bovine serum (FBS), 10% (v/v) WEHI-3BD conditioned medium, 100 U/mL penicillin and 100 µg/mL streptomycin. WEHI-3BD cells were maintained in RPMI 1640 medium supplemented with 2 g/L sodium bicarbonate, 10% (v/v) FBS, 100 U/mL penicillin and 100 µg/mL streptomycin, and the conditioned medium was collected three times per week and stored at -20 °C until it was required. For the mitogenic assays, the BaF32 cells were transferred into IL-3 depleted medium for 24 h prior to experimentation and seeded into 96-well plates at a density of 2×10^4 cells/well in the presence of medium only, 30 nM heparin, CH-Arg, S-CH-Arg or 2NS-CH-Arg either in the presence or absence of 0.03 nM FGF-2. Cells exposed to

heparin and FGF-2 were used as a positive control for the assay, as this combination is known to induce cell proliferation, while cells exposed to each of the treatments in the absence of FGF-2 were used as a negative controls. Background absorbance readings were also obtained for each of the treatments in the absence of cells. Cells were incubated for 96 h in 5% CO_2 at 37 °C, and the number of cells present was assessed using the MTS assay. The MTS reagent (Promega, Madison, USA) was added to the cell cultures 6 h prior to measurement of the absorbance at 490 nm.

Isolation of human fetal chondroblasts

Human fetal knee joint rudiment cells were isolated from cartilage as described previously.[19] The isolated rudiment cells were cultured in DMEM culture medium supplemented with 2 mM L-glutamine, 50 µg/mL L-ascorbic acid, 1% (v/v) penicillin/streptomycin and 10% (v/v) fetal calf serum (FCS) and used for experiments at passage 2.

Cell proliferation analysis

Human fetal chondroblasts were seeded in 6-well tissue culture polystyrene plates at a density of 2×10^5 cells/well in 3 mL medium. Cells were incubated for 4 h prior to the addition of CH-Arg, S-CH-Arg or 2NS-CH-Arg (10 µg/mL). Cell viability was analysed at 24, 48 and 72 h after the addition of CH-Arg, S-CH-Arg or 2NS-CH-Arg using an automated cell viability analyser (ViCell, Beckman Coulter, Sydney, Australia) that is based on trypan blue exclusion dye analysis.

Immunocytochemistry

Human fetal chondroblasts were cultured to confluence on microscope slides (Ultrafrost, Lomb Scientific), fixed with ice cold acetone for 3 min and rinsed with 50 mM Tris-HCl, 0.15 M NaCl, pH 7.6 (TBS). Slides were then blocked with 0.1% w/v casein in TBS for 1 h at room temperature (RT) followed incubation with the primary antibodies for 16 h at 4 °C. Primary antibodies were used against collagen type I (clone I-8H5, 4 µg/ml), collagen type II (clone II-4C11, 4 µg/ml), aggrecan (clone 969D4D11, 0.2 µg/ml) and perlecan (CCN-1, 1:1000). Slides were rinsed twice with TBS containing 0.1 % (w/v) Tween-20 (TBST) and incubated with the biotinylated anti-mouse or anti-rabbit secondary antibodies (1:500) for 1 h at RT before rinsing twice with TBST and incubation with SA-FITC (1:250) for 30 min at RT followed by four rinses with TBST. The slides were then counterstained with 1 µg/mL of 4′, 6-diamidino-2-phenylindole, dilactate (DAPI, Life Technologies, Carlsbad, CA, USA) in PBS for 10 min in the dark and rinsed four times with the deionized water before imaging using a fluorescence microscope (Zeiss Axioskop Mot Mat 2, Sydney, Australia).

Quantitative real-time PCR

Total RNA was isolated from cells using TRI Reagent (1 mL per 10^7 cells) and then treated with DNase using the RQ1 RNase-Free DNase kit (Promega) to remove contaminating DNA. Subsequently, 1 µg RNA was transcribed into cDNA using oligo d(T)23 primer mix (ProtoScript® M-MuLV First Strand cDNA synthesis kit, GeneSearch Pty Ltd, Arundel, Australia). For quantitative real-time PCR (qPCR), 1µL cDNA was mixed with 0.5 µl forward and reverse primers (10 µM each, Table 1) and 10 µL Power SYBR Green PCR Master Mix (Applied Biosystems, Mulgrave, Australia) followed by adding RNAase free water to make up to 20 µL per sample. GAPDH was used as an endogenous control and to normalise the results for each of the primer sets. Samples were subject to 40 reactions using the ABI StepOne™ Real-time PCR system.

Table 1. qPCR primers

Gene	Accession number	Forward primer (5'-3')	Reverse primer (5'-3')
Chondrogenic			
Collagen type II	NM_001844	ACACTGCCAACG TCCAGATGAC	CAGTGTACGT GAACCTGCTAT TGC
Aggrecan	NM_001135	TGTCCAAGGAGA AGGAGGTAGTG	GATGCCTTTCA CCACGACTTC
Perlecan	NM_005529	GGTGCCAGAGCG GGTG	CTGCATCGAA CCGGAACTC
SOX-9	NM_000346	CCCGCTCACAGT ACGACTAC	CTGTGTGTAGA CGGGTTGTTC
Osteogenic			
Collagen type I	NM_000088	TAAAGGGTCACC GTGGCTTCTC	GCAGGAAGCT GAAGTCGAAA CC
Alkaline phosphatase	NM_000478	AGGGCTGTAAGG ACATCGCCTA	GCGGTTCCAG ATGAAGTGGG A
Osteocalcin	NM_199173	CGAGGTAGTGAA GAGACCCA	GTGGTCAGCC AACTCGTCAC
Osteopontin	NM_001040058	CATGTGGACAGC CAGGACTC	TGTGAGGTGA TGTCCTCGTC
Growth factors and antagonists			
BMP2	NM_00120	GGTTCAACCCCA GCACATGAAGT	GCTGCGTGTTG GGCAAAAAGT
Noggin	NM_005450	GCGGCCAGCACT ATCTCCACAT	GCACGGAGCA CGAGCGCTTA

Statistical Analyses

A two-way analysis of variance (ANOVA) was performed to compare multiple conditions while a student's t test (two samples, two tailed distribution assuming equal variance) was used to compare statistical significance between two conditions. Results of $p < 0.05$ were considered significant. Experiments were performed in triplicate and experiments were repeated twice.

Results

Characterization of sulfated CH-Arg

The sulfate modification steps aimed to sulfate CH-Arg at positions C2, C3 and C6 using the homogeneous sulfation method and at position C2 using the 2-N sulfation method are outlined in Fig. 1. Sulfate modification of CH-Arg was verified by ATR-FTIR (Fig. 2) Adsorption bands at 1230 and 800 cm^{-1} indicated the presence of S=O and C–O–S, respectively, suggesting that CH-Arg was successfully modified. The S=O

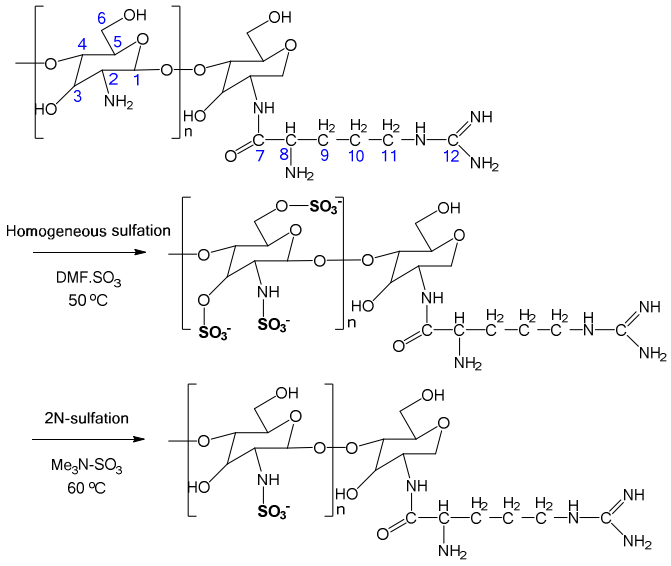

Figure 1. Schematic of sulftion of CH-Arg homogeneous and 2N-sulfation.

adsorption band was observed for the 2N-sulfated CH-Arg (2NS-CH-Arg), however this band was masked for the homogeneously sulfated CH-Arg (S-CH-Arg) (Fig. 2A). The loss of the adsorption band at 1590 cm^{-1} in the sulfated CH-Arg samples indicated the modification of the NH_2 groups, whilst the appearance of the band at 1550 cm^{-1} indicated the formation of N–H bonds. Additionally, changes in the adsorption bands at 1154 and 1028 cm^{-1} were observed for the sulfate modified CH-Arg that corresponded to C–O–C (glycosidic linkage) and C–O stretching, respectively (Fig. 2A).

The surface spectra of CH-Arg, S-CH-Arg and 2NS-CH-Arg confirmed the presence of carbon, nitrogen and oxygen in each of the materials and the presence of sulfur in both S-CH-Arg and 2NS-CH-Arg with a higher level of sulfur substitution evident in the 2NS-CH-Arg (Fig. 2 B and Table 2). Elemental analysis was performed to obtain the degree of sulfation of each of the materials (Table 2). A background level of sulfur was found in CH-Arg being 0.1%. The sulfur contents of S-CH-Arg and 2NS-CH-Arg were 1.6 and 2.5 %, respectively. The degree of sulfation for S-CH-Arg and 2NS-CH-Arg were 6.2 and 8.9 %, respectively. These data indicated that both methods of sulfation were successful and that the 2NS-CH-Arg had the highest level of sulfur substitution. When the homogeneous sulfation reaction was performed with enough $DMF.SO_3$ to modify half of the available N and O positions susceptible to sulfate modification, a degree of sulfation of 4% was achieved, indicating that sulfate substitution of CH-Arg could be controlled. However, varying the reaction time from 1 – 3 h had no effect on the level of homogeneous sulfation achieved.

The HSQC spectra from 2D NMR were also used to investigate the sulfate functionalization of the CH-Arg materials (Fig. 3). Peak shifts were observed for the homogeneously sulfated CH-Arg at the C_2 position (y axis) and the H_1 peaks assigned to GlcNAc H_2 and GlcNAc H_3 indicating that these residues had been sulfated (Fig. 3A). This peak shift was also observed for

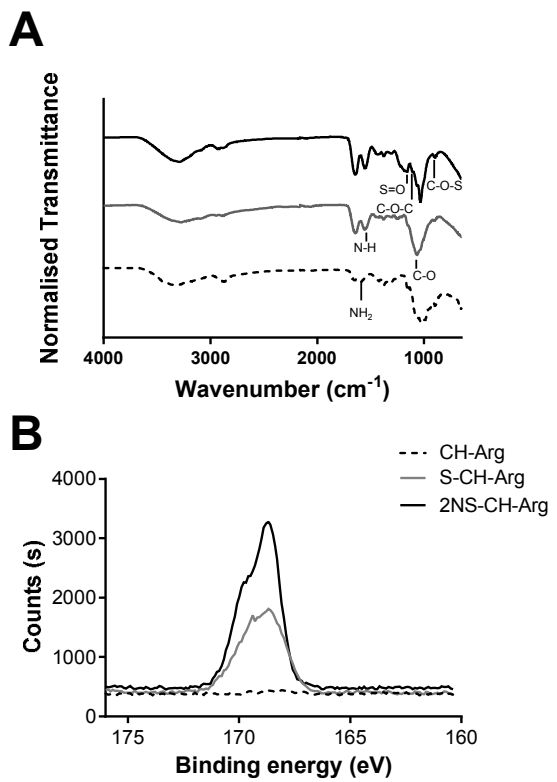

Figure 2. (A) ATR-FTIR and (B) XPS spectra of CH-Arg, S-CH-Arg and 2NS-CH-Arg.

Table 2. The elemental content of CH-Arg, S-CH-Arg and 2NS-CH-Arg.

Sample	Element content (%)				Degree of sulfation (%)
	C	N	O	S	
CH-Arg	60.9	7.2	31.9	0.1	0.6
S-CH-Arg	55.6	11.3	31.4	1.6	6.2
2NS-CH-Arg	53.0	12.1	30.9	2.5	8.9

the 2NS-CH-Arg, however to a lesser extent than the S-CH-Arg (Fig. 3). No species were found in the region of C_3S or C_6S indicating that the homogeneous sulfation method did not modify the CH-Arg with 3-O or 6-O-sulfation. The HSQC spectra from 2D NMR were also used to investigate whether the NH_2 groups on arginine were modified by the sulfation reactions. The signal at 57 ppm can be attributed to both C2 on chitosan and C8 on arginine. The protons at the C2 on chitosan at 3.5 ppm shifted after sulfate modification, while the protons on C8 of arginine at 3.7 ppm did not, indicating that the NH_2 group on chitosan was modified while the NH_2 on arginine C8 was not modified. An additional NH_2 is located on C12 of arginine that can be attributed to 159 ppm on the ^{13}C spectra. A peak was detected at 159 ppm in the CH-Arg and the sulfated CH-Arg, however an additional peak was detected at 169 ppm which may be due to modification of the C12 with sulfate (data not shown).

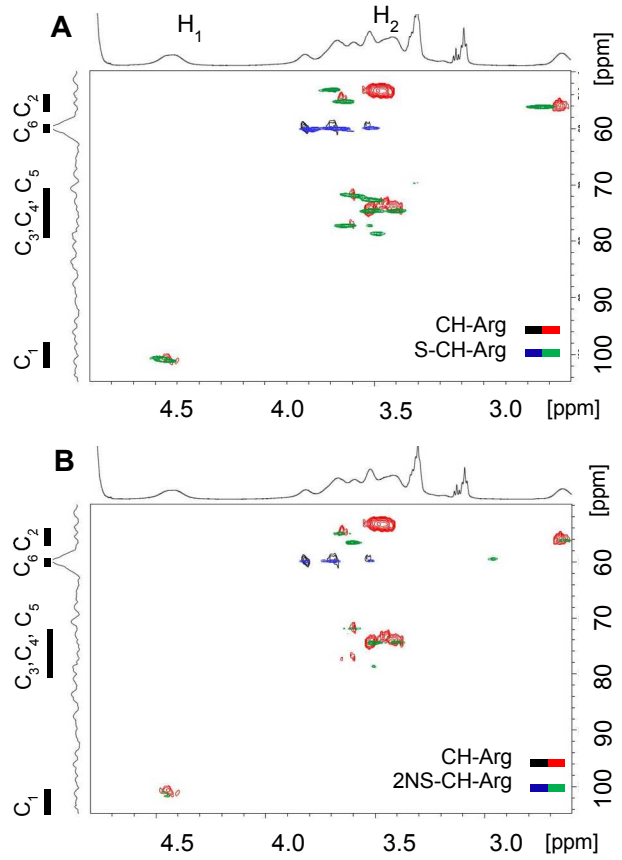

Figure 3. HSQC NMR spectra of (A) CH-Arg and S-CH-Arg and (B) CH-Arg and 2NS-CH-Arg in D_2O at 298 K.

Growth factor binding and signalling activity of sulfated CH-Arg

The BaF32 cell assay was used to analyze the activity of the CH-Arg and sulfated CH-Arg utilizing the well-characterized formation of biologically active ternary complexes between heparin, FGF-2 and FGFR1c present on the cell surface that resulted in the proliferation of the BaF32 cells that could be measured by the MTS assay after 96 h. Neither the CH-Arg, the S-CH-Arg nor the 2NS-CH-Arg were found to significantly (p<0.05) alter the absorbance values compared to that of medium only indicating that the materials did not interfere with the MTS assay (Fig. 4). The positive control for the assay was the FGFR1c expressing cells exposed to heparin and FGF-2 as shown by the significant (p<0.05) increase in absorbance compared to cells exposed to heparin only (Fig. 4). The negative controls for the assay were cells exposed to each of the negative controls for the assay were cells exposed to each of the treatments in the absence of FGF-2. Neither CH-Arg alone nor in the presence of FGF-2 promoted the proliferation of the FGFR1c expressing BaF32 cells. BaF32 cells exposed to either S-CH-Arg or 2NS-CH-Arg alone also did not promote the proliferation of the cells, however, when cells were exposed to these materials in the presence of FGF-2 the cells proliferated to a significantly higher (p<0.05) extent. This indicated that S-CH-Arg and 2NS-CH-Arg formed active ternary complexes with FGF-2 and FGFR1c.

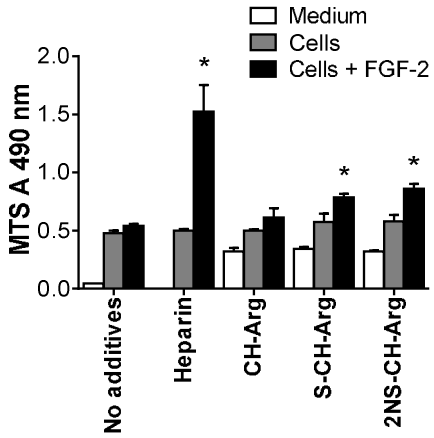

Figure 4. Activity of CH-Arg, S-CH-Arg and 2NS-CH-Arg determined by the signalling of FGFR1c expressing BaF32 cells in the presence of FGF2 as measured by cell number by the MTS assay. Cells in the presence of FGF2 and heparin were used as a control for the formation of active heparin containing ternary complexes. Data presented as mean ± standard deviation (n = 3). * Indicated significant differences (p<0.05) within treatments for cells and FGF2 compared to cells only as determined by a two-way ANOVA.

The effect CH-Arg, S-CH-Arg and 2NS-CH-Arg on primary human chondroblast proliferation was analyzed at a concentration of 10 µg/mL over a period of 7 days (Fig. 5). CH-Arg, S-CH-Arg did not significantly (p<0.05) alter the proliferation of the cells compared to cells exposed to medium only. In contrast, the proliferation of chondroblast cells exposed to 10 µg/mL 2NS-CH-Arg exhibited significantly (p<0.05) reduced cell proliferation after 3 and 7 days of exposure compared to cells exposed to medium only. The observed reduction in cell proliferation when exposed to 2NS-CH-Arg was not to the extent that is considered cytotoxic being at most a 15 % decrease in proliferation. As S-CH-Arg had no effect on cell proliferation it was carried forward into studies of the osteo- and chondro-genic potential.

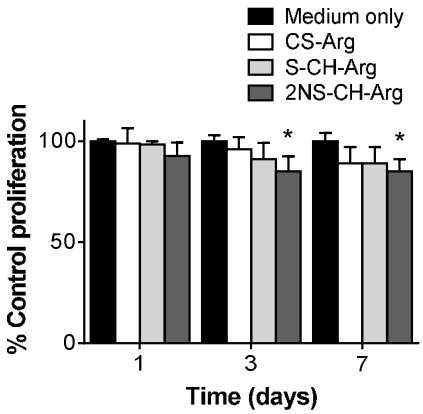

Figure 5. Proliferation of human chondroblasts over a period of 7 days exposed to CH-Arg, S-CH-Arg and 2NS-CH-Arg at a concentration of 10 µg/mL measured by the MTS assay. Data presented at mean ± standard deviation (n = 3). * indicated significant difference (p<0.05) compared with cells exposed to medium only at each time point as determined by a two-way ANOVA.

Osteogenic and chondrogenic potential of CH-Arg and S-CH-Arg

The expression of osteo- and chondro-genic genes by cells exposed to CH-Arg or S-CH-Arg for a period of 1, 3 or 7 days was analyzed by isolating mRNA and performing quantitative real time PCR (qPCR) over 40 cycles compared to GAPDH expression at each time point for each condition (Figs. 6-8).

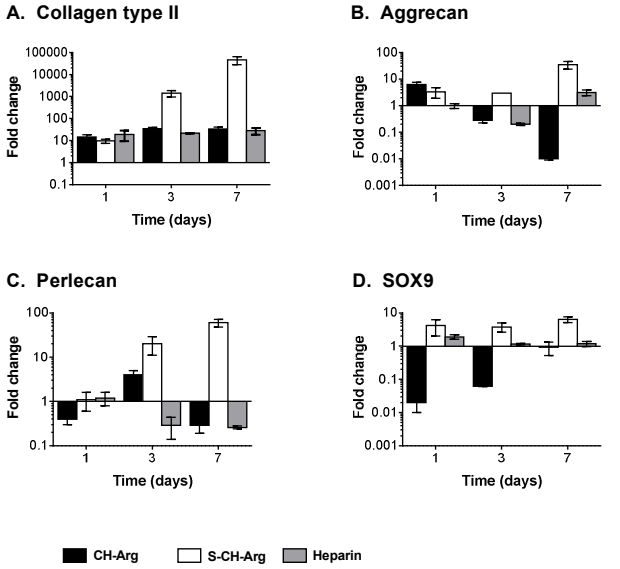

Figure 6. Quantitative PCR analysis of (A) collagen type II, (B) aggrecan, (C) perlecan and (D) SOX9 gene expression in human fetal chondroblasts exposed to CH-Arg (black), S-CH-Arg (white) or heparin (grey) for up to 7 days. Data presented a fold change compared to cells exposed to medium only and corrected for GAPDH expression for each treatment.

Cells were also analyzed at each of these time points after exposure to heparin, as a control for exposure to a sulfated glycosaminoglycan, and medium only. Genes involved in chondrogenic expression including collagen type II, aggrecan, perlecan and SOX-9 were investigated. Cells exposed to either CH-Arg or heparin displayed a 14 - 30 fold increase in collagen type II gene expression over the 7 day analysis period compared to cells exposed to medium only. In contrast, cells exposed to S-CH-Arg displayed an increase in collagen type II gene expression over the 7 day analysis period with a 45,000 fold increase compared to cells exposed to medium only after 7 days and significantly (p<0.05) higher expression compared to cells exposed to CH-Arg (Fig. 6A). Cells exposed to CH-Arg displayed a decrease in aggrecan gene expression over the 7 day analysis period compared to cells exposed to medium only while cells exposed to heparin displayed a 3 fold increase in aggrecan gene expression compared to cells exposed to medium only after 7 days (Fig. 6B). In contrast, cells exposed to S-CH-Arg displayed a 3 fold increase in aggrecan gene expression after 1 and 3 days and a 35 fold increase after 7 days of exposure compared to cells exposed to medium only. A similar pattern for perlecan gene expression was observed with both CH-Arg and heparin down regulating perlecan gene expression after 7 days while cells exposed to S-CH-Arg displayed a 60 fold increase in gene expression compared to cells exposed to medium only after 7 days (Fig. 6C). Cells exposed to either CH-Arg or heparin either did not change the level of expression or reduced the level of expression of SOX-9 over the 7 day analysis period compared to cells exposed to medium only (Fig. 6D). In contrast, cells exposed to S-CH-Arg displayed a 4-6 fold increase in SOX-9 expression over the 7 day analysis period compared to cells exposed to medium only. Together these data indicate that S-CH-Arg significantly (p<0.05) upregulated chondrogenic gene expression compared to cells exposed to CH-Arg or heparin over a period of 7 days.

Genes involved in osteogenic expression including collagen type I, alkaline phosphatase, osteocalcin and osteopontin were also investigated by qPCR. Cells exposed to CH-Arg displayed an 80-500 fold increase in collagen type I gene expression after 3 and 7 days exposure compared to cells exposed to medium only (Fig. 7A). In contrast, cells exposed to either S-CH-Arg or heparin displayed a decrease in collagen type I gene expression over the 7 day analysis period. Cells exposed to CH-Arg displayed an increase in alkaline phosphatase gene expression at a maximum of 70 fold increase in gene expression over the 7 day analysis period compared to cells exposed to medium only (Fig. 7B). Cells exposed to heparin or S-CH-Arg did not increase their gene expression levels above that of cells exposed to medium only over 7 days (Fig. 7 B). Cells exposed to CH-Arg also significantly (p<0.05) increased their expression of osteocalcin and osteopontin compared to cells exposed to medium only (Fig. 7C and D). In contrast, cells exposed to S-CH-Arg or heparin either displayed the same level or reduced expression of osteocalcin and osteopontin compared to cells exposed to medium only. Together these data indicated that CH-Arg promoted osteogenic gene expression while cells

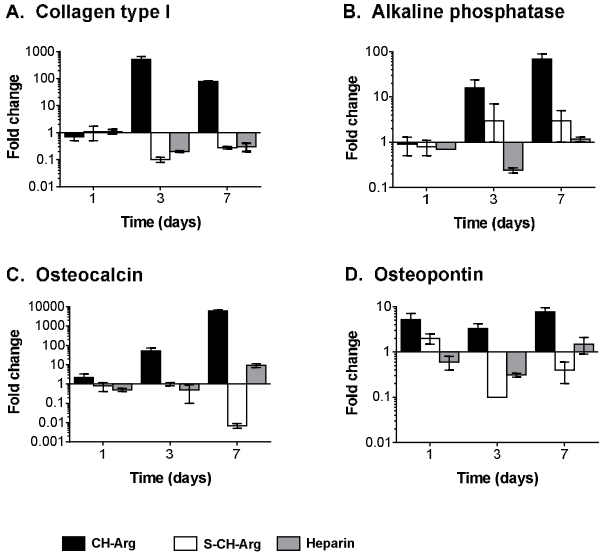

Figure 7. Quantitative PCR analysis of (A) collagen type I, (B) alkaline phosphatase, (C) osteocalcin and (D) osteopontin gene expression in human fetal chondroblasts exposed to CH-Arg (black), S-CH-Arg (white) or heparin (grey) for up to 7 days. Data presented a fold change compared to cells exposed to medium only and corrected for GAPDH expression for each treatment.

exposed to S-CH-Arg or heparin over a period of 7 days did not express osteogenic genes.

The level of gene expression for BMP-2 was also analysed as this growth factor promotes osteogenesis. Cells exposed to CH-Arg were found to display significantly (p<0.05) higher levels of the BMP-2 gene expression compared to cells exposed to medium only, S-CH-Arg or heparin (Fig. 8A). The level of gene expression for the BMP antagonist, noggin, was found to be down-regulated in cells exposed to either CH-Arg or heparin which would allow the signalling of BMPs, while it was up-regulated in cells exposed to S-CH-Arg further indicating the S-CH-Arg was able to inhibit the osteogenic phenotype in these cells (Fig. 8 B).

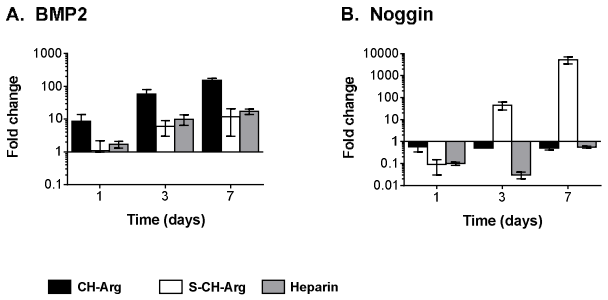

Figure 8. Quantitative PCR analysis of (A) BMP-2 and (B) noggin gene expression in human fetal chondroblasts exposed to CH-Arg (black), S-CH-Arg (white) or heparin (grey) for up to 7 days. Data presented a fold change compared to cells exposed to medium only and corrected for GAPDH expression for each treatment.

When the human fetal chondroblast cells were exposed to either CH-Arg or medium only for 7 days they expressed detectable levels of type I collagen (Fig. 9A and D (i)) as well as aggrecan (Fig. 9A and D (iii)) that was located intracellularly and perlecan (Fig. 9A and D (iv)) that was detected as micro-fibrillar structures in both the pericellular and extracellular matrices. This was indicative of the de-differentiated phenotype of chondrocytes when maintained as monolayer cultures. Cells exposed to heparin also expressed collagen type I, aggrecan and perlecan with a similar distribution to that observed for cells exposed to CH-Arg or medium only (Fig. 9C (i, iii and iv)), however both collagen type I and perlecan were present as more discrete fibrillated structures. In contrast, cells exposed to S-CH-Arg expressed collagen types I and II, aggrecan and perlecan (Fig. 9 B). Collagen types I and II and perlecan were detected as micro-fibrillar structures while aggrecan was detected intracellularly.

Discussion

Chitosan has been investigated for a range of biomedical applications due to its cytocompatibility, anti-microbial property and ease of fabrication into various scaffolds, nanoparticles, fibres or surfaces, and is often used in combination with other materials to improve its mechanical properties.[30, 31] Water-soluble forms of chitosan, such as CH-Arg, circumvent the need to provide aqueous acidic conditions for chitosan to be soluble, while sulfated forms of chitosan have started to attract research attention for their ability to mimic the extent of sulfation of natural glycosaminoglycans. Arginine functionalized chitosan has been reported previously and synthesized using a non-protected arginine that results in the chitosan backbone being randomly substituted with poly(arginine) chains with an overall positive charge in neutral conditions.[10, 13] The chitosan (poly)arginine material is thus expected to possess different biological properties from the chitosan-arginine used in this study. The chitosan-arginine utilized in this study was synthesized using conditions to obtain single arginine residues covalently linked to the chitosan backbone.[8, 15]

In this study the sulfation of CH-Arg is reported for the first time and was achieved with a sulfur substitution up to 9 %. Chitosan with molecular weights between 50 and 300 kDa has been sulfated at the 2-N and 6-O positions with sulfur substitution up to 14 %.[24, 32] Previous reports have shown that chitosan can be sulfated at positions C2 and C6 resulting in 2-N and 6-O sulfation, respectively,[24] however in this study sulfation was only achieved at the 2-N position. The organic solvents used for the sulfation of the water soluble CH-Arg may have reduced the solubility of the CH-Arg leading to lower levels of sulfation and no modification at the 6-O position. Additionally, the sulfate substitution of arginine cannot be excluded. Heparan sulfate is approximately 5–10 % substituted with sulfur,[33] indicating that the sulfated chitosans produced in this study were comparable to the level of sulfation of heparan sulfate and hence are in the sulfation level range to be biomimetic and bioactive.

Sulfated forms of chitosan have been investigated as growth factor delivery vehicles such as loaded with BMP-2 to promote an osteogenic phenotype in various cell lines and animal models[24-26, 34] or FGF-2 to promote cell proliferation.[35] Additionally, chitosan (poly)arginine has been explored for intracellular gene and drug delivery.[10, 36] This study sought to investigate the inherent growth factor binding and signaling activity of the sulfated CH-Arg using the BaF32 cell proliferation assay in the presence of FGF-2. Both S-CH-Arg and 2NS-CH-Arg were found to be active in the BaF32 cell assay, indicating their ability to bind and potentiate the signaling of FGF-2. CH-Arg did not signal FGF-2, and might be expected as its overall positive charge does not mimic a negatively charged heparin molecule known to bind FGF-2.[37] However, the level of activity of the sulfated CH-Arg was not to the same level as heparin when used at the same concentration, and may be expected due to the lower level of sulfur substitution than heparin. Additionally, the pattern of sulfation along the CH-Arg chain may have affected the level of growth factor binding and signaling. Heparin and heparan sulfate bind to FGF-2 through a minimum of a hexasaccharide sequence while a tetrasaccharide sequence is required for signaling as the longer chain is needed to bridge the distance

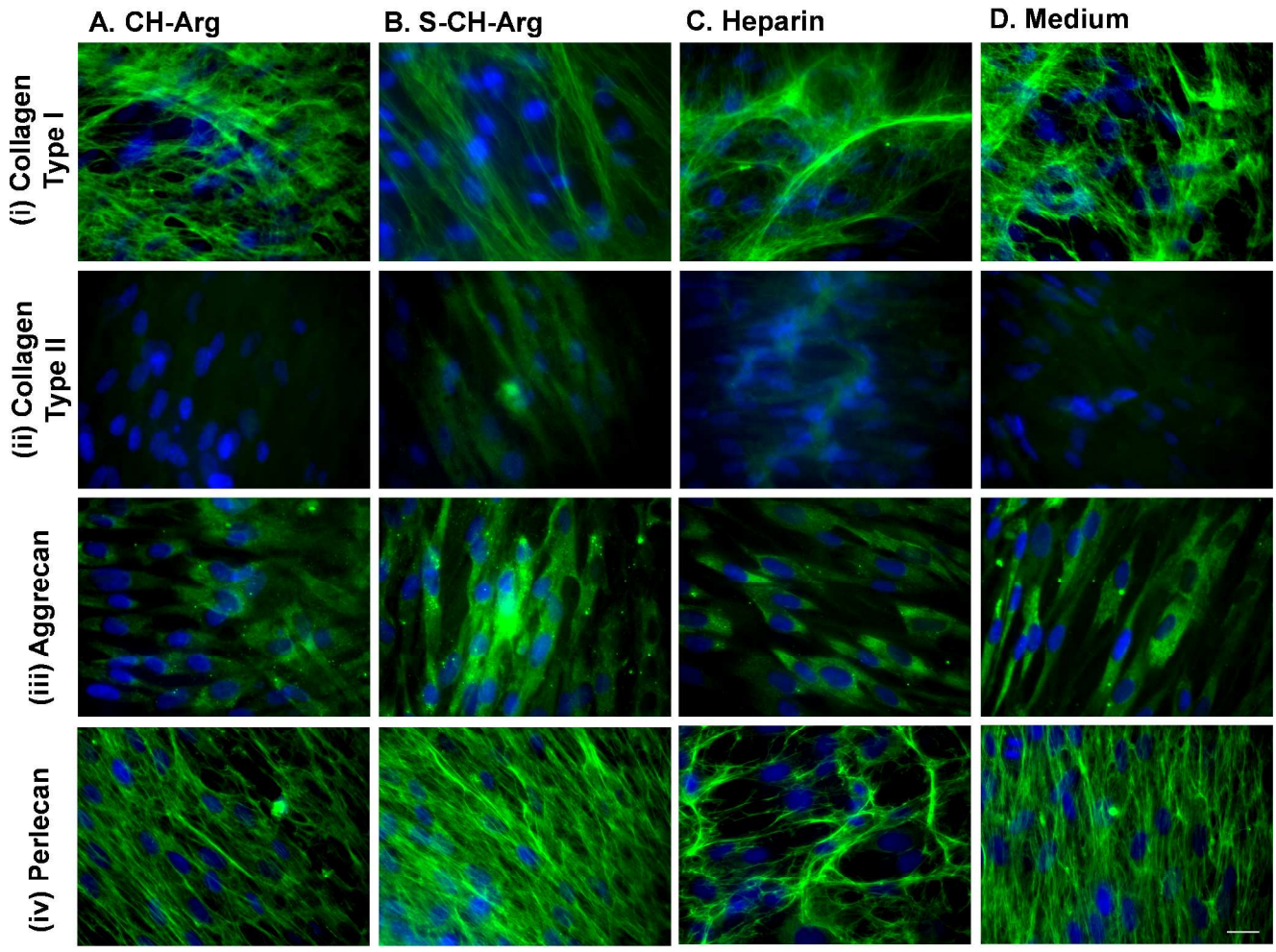

Figure 9. Immunolocalisation of (i) collagen type I (Ab II-4C11), (ii) collagen type II (Ab I-8H5), (iii) aggrecan (Ab 969D4D) and (iv) perlecan (CCN-1) in human fetal chondroblasts exposed to (A) CH-Arg, (B) S-CH-Arg, (C) heparin or (D) medium for 7 days. Specific staining was shown by FITC (green) and cell nuclei were counterstained with DAPI (blue). The scale bar represents 20 μm.

between the growth factor and its cognate receptor.[37] This implies that the sulfated CH-Arg contained sulfation patterns that represented these natural sulfation patterns in heparin and heparan sulfate.

The osteogenic activity of sulfated chitosan has been investigated previously when loaded with BMP-2.[24-26, 34] BMP-2 is one of the most effective inducers of osteogenic differentiation to promote bone regeneration.[38] However the application of BMPs in various adjuvants or scaffolds has many drawbacks as high doses can lead to bone resorption or ectopic ossification.[39] Chitosan itself has been investigated for its osteogenic potential,[40] however is most often investigated when part of a composite material to improve osteogenic activity whilst relying on the other components of the composite to provide mechanical properties.[41-44] This study demonstrated for the first time that arginine functionalized chitosan alone supported the osteogenic differentiation of human fetal progenitor cells over a period of 7 days through the upregulation of osteogenic genes including collagen type I, alkaline phosphatase, osteocalcin and osteopontin. Additionally, treatment of the progenitor cells with CH-Arg promoted BMP-2 gene expression and the down-regulation of noggin, further supporting the osteoblastic phenotype of the cells in contact with CH-Arg and the inherent osteogenic capacity of this material in the absence of exogenous growth factors. These data are in line with other studies that have investigated the osteogenic potential of chitosan-based materials in contact with progenitor cells [45-48] and *in vivo*,[49] however this study has demonstrated for the first time that a water soluble form of chitosan alone can promote the osteogenic phenotype of human progenitor cells.

Chitosan functionalized with chondroitin and dermatan sulfate has been shown to maintain the chondrogenic phenotype of rat chondrocytes [50, 51] while a chitosan composite containing chitin and heparin was also able to maintain the chondrogenic phenotype of bovine chondrocytes.[52] Thus sulfated polysaccharide structures can maintain the chondrogenic phenotype as demonstrated in this study. In contrast, other studies have shown that chitosan can support both the

chondrocyte phenotype and proliferation in the absence of sulfated polysaccharides, but in the presence of chondrogenic medium.[52] Additionally, chitosan sponges in the presence of hyaluronan, an unsulfated glycosaminoglycan, can support the cartilage phenotype of murine bone marrow mesenchymal stem cells[53] or bovine chondrocytes when grown in chondrogenic medium.[54] This study demonstrated for the first time that sulfated chitosan-arginine supports the chondrogenic differentiation of human fetal progenitor cells over a period of 7 days through the up-regulation of chondrogenic genes including collagen type II, aggrecan, perlecan and SOX9 in the absence of exogenous chondrogenic-inducing compounds.

Conclusions

This study demonstrated for the first time that arginine functionalized chitosan could be functionalized with sulfate groups to replicate the degree of sulfation of naturally occurring glycosaminoglycans. The sulfated chitosan-arginine materials were able to bind and signal FGF-2 indicating their ability to modulate the activity of growth factors. Chitosan-arginine was found to promote an osteogenic phenotype in primary human chondroblast cells in the absence of osteogenic medium over a period of 7 days, while sulfated chitosan-arginine was able to promote a chondrogenic phenotype in these same cells over the same time period in the absence of chondrogenic medium. Together these data demonstrate the fine control of the bone and cartilage phenotype that can be obtained from sulfate modified water soluble chitosan that mimic natural growth factor binding glycosaminoglycans. While the results presented in this study are promising osteo-chondral repair using human progenitor cell *in vitro,* in the future these materials will be investigated further for clinical application in an osteo-chondral defect model *in vivo* as well as analyses of the material degradation and clearance.

Acknowledgements

This work was supported by funding from the Australian Research Council under the Linkage Project (LP100100504) scheme. The authors would also like to acknowledge the UNSW Mark Wainwright Analytical Centre for assistance with NMR analysis.

Notes and references

[a] Graduate School of Biomedical Engineering. The University of New South Wales, Sydney, NSW 2052, Australia.

[b] Synedgen Inc, Claremont, CA, USA.

[*] Corresponding Author: Tel.: +61 2 9385 3910; fax: +61 2 9663 2108. *E-mail address*: m.lord@unsw.edu.au (M.S. Lord).

[#] Present address: Centre for Health Technologies, University of Technology, Sydney, Ultimo, NSW 2007, Australia.

1 R. A. A. Muzzarelli, *Carbohydr Polym*, 2009, **76**, 167-182.
2 S. K. Shukla, A. K. Mishra, O. A. Arotiba and B. B. Mamba, *Int J Biol Macromol*, 2013, **59**, 46-58.
3 R. A. Lahmer, A. P. Williams, S. Townsend, S. Baker and D. L. Jones, *Food Control*, 2012, **26**, 206-211.
4 M. S. Lord, B. Cheng, S. J. McCarthy, M. Jung and J. M. Whitelock, *Biomaterials*, 2011, **32**, 6655-6662.
5 K. Murakami, H. Aoki, S. Nakamura, S. i. Nakamura, M. Takikawa, M. Hanzawa, S. Kishimoto, H. Hattori, Y. Tanaka, T. Kiyosawa, Y. Sato and M. Ishihara, *Biomaterials*, 2010, **31**, 83-90.
6 H. K. No, N. Young Park, S. Ho Lee and S. P. Meyers, *Int J Food Microbiol*, 2002, **74**, 65-72.
7 T. Takei, H. Nakahara, H. Ijima and K. Kawakami, *Acta Biomater*, 2012, **8**, 686-693.
8 H. Tang, P. Zhang, T. L. Kieft, S. J. Ryan, S. M. Baker, W. P. Wiesmann and S. Rogelj, *Acta Biomater*, 2010, **6**, 2562-2571.
9 L. Casettari, D. Vllasaliu, J. K. W. Lam, M. Soliman and L. Illum, *Biomaterials*, 2012, **33**, 7565-7583.
10 Y. Gao, Z. Xu, S. Chen, W. Gu, L. Chen and Y. Li, *Int J Pharm*, 2008, **359**, 241-246.
11 S. Park, S. K. Lee and K. Y. Lee, *J Control Release*, 2011, **152**, e165-166.
12 J. Suwan, Z. Zhang, B. Li, P. Vongchan, P. Meepowpan, F. Zhang, S. A. Mousa, S. Mousa, B. Premanode, P. Kongtawelert and R. J. Linhardt, *Carbohydr Res*, 2009, **344**, 1190-1196.
13 B. Xiao, Y. Wan, M. Zhao, Y. Liu and S. Zhang, *Carbohydr Polym*, 2011, **83**, 144-150.
14 H. X. Lv, Z. H. Zhang, X. P. Wang, Q. Q. Cheng, W. Wang, X. H. Huang, J. P. Zhou, Q. Zhang, L. L. Hou and W. Huo, *Molecules*, 2011, **16**, 6778-6790.
15 S. Baker, W. P. Wisemann and S. Ryan, ed. I. Synedgen, Baker, S. Wisemann, W.P. Ryan, S., USA, 2007.
16 J. M. Whitelock and R. V. Iozzo, *Chem Rev*, 2005, **105**, 2745-2764.
17 R. Huang, Y. Du, J. Yang and L. Fan, *Carbohydr Res*, 2003, **338**, 483-489.
18 Y. C. Ho, S. J. Wu, F. L. Mi, Y. L. Chiu, S. H. Yu, N. Panda and H. W. Sung, *Bioconjug Chem*, 2010, **21**, 28-38.
19 C. Y. Chuang, K. Shahin, M. S. Lord, J. Melrose, P. M. Doran and J. M. Whitelock, *Biomaterials*, 2012, **33**, 4078-4088.
20 R. R. Gomes, M. C. Farach-Carson and D. D. Carson, *Cells Tissues Organs*, 2004, **176**, 79-86.
21 W. Yang, R. R. Gomes, A. J. Brown, A. R. Burdett, M. Alicknavotch, M. C. Farach-Carson and D. D. Carson, *Tissue Eng*, 2006, **12**, 2009-2024.
22 H. Munakata, K. Takagaki, M. Majima and M. Endo, *Glycobiology*, 1999, **9**, 1023-1027.
23 V. F. Sechriest, Y. J. Miao, C. Niyibizi, A. Westerhausen-Larson, H. W. Matthew, C. H. Evans, F. H. Fu and J. K. Suh, *J Biomed Mater Res*, 2000, **49**, 534-541.
24 H. Zhou, J. Qian, J. Wang, W. Yao, C. Liu, J. Chen and X. Cao, *Biomaterials*, 2009, **30**, 1715-1724.
25 D. Peschel, K. Zhang, S. Fischer and T. Groth, *Acta Biomater*, 2012, **8**, 183-193.
26 J. Zhao, G. Shen, C. Liu, S. Wang, W. Zhang, X. Zhang, X. Zhang, D. Ye, J. Wei, Z. Zhang and X. Jiang, *Tissue Eng Part A*, 2012, **18**, 185-197.
27 J. M. Whitelock, L. D. Graham, J. Melrose, A. D. Murdoch, R. V. Iozzo and P. A. Underwood, *Matrix Biol*, 1999, **18**, 163-178.
28 D. M. Ornitz, J. Xu, J. S. Colvin, D. G. McEwen, C. A. MacArthur, F. Coulier, G. Gao and M. Goldfarb, *J Biol Chem*, 1996, **271**, 15292-15297.
29 D. M. Ornitz, A. Yayon, J. G. Flanagan, C. M. Svahn, E. Levi and P. Leder, *Mol Cell Biol*, 1992, **12**, 240-247.
30 R. A. A. Muzzarelli, *Carbohydr Polym*, 2011, **83**, 1433-1445.
31 R. A. A. Muzzarelli, F. Greco, A. Busilacchi, V. Sollazzo and A. Gigante, *Carbohydr Polym*, 2012, **89**, 723-739.
32 R. Xing, S. Liu, H. Yu, Z. Guo, Z. Li and P. Li, *Carbohydr Polym*, 2005, **61**, 148-154.
33 D. J. Langeslay, C. N. Beeer, A. Naggi, M. Guerrini, G. Torri and C. K. Larive, *Anal Chem*, 2013, **85**, 1247-1255.
34 L. Cao, J. Wang, J. Hou, W. Xing and C. Liu, *Biomaterials*, 2014, **35**, 684-698.
35 A. Weltrowski, M. L. da Silva Almeida, D. Peschel, K. Zhang, S. Fischer and T. Groth, *Macromol Biosci*, 2012, **12**, 740-750.
36 L. L. Cai, O. Liu, X. Li, X. H. Huang, Y. Q. Ye, F. Y. Chen, H. Yuan, F. Q. Hu and Y. Z. Du, *Int J Nanomed*, 2011, **6**, 3499-3508.
37 J. E. Turnbull, D. G. Fernig, Y. Ke, M. C. Wilkinson and J. T. Gallagher, *J Biol Chem*, 1992, **267**, 10337-10341.

38 A. L. Jones, R. W. Bucholz, M. J. Bosse, S. K. Mirza, T. R. Lyon, L. X. Webb, A. N. Pollak, J. D. Golden and A. Valentin-Opran, *J Bone Joint Surg Am*, 2006, **88**, 1431-1441.
39 D. W. Benglis, M.Y. and A. D. Levi, *Neurosurgery*, 2008, **62**, ONS423-431.
40 P. R. Klokkevold, L. Vandemark, E. B. Kenney and G. W. Bernard, *J Periodontol,* 1996, **67**, 1170-1175.
41 W. W. Thein-Han and R. D. K. Misra, Acta Biomater, 2009, 5, 1182-1197.
42 J. R. Zhang, J. Nie, Q. Zhang, Y. Li, Z. Wang and Q. Hu, *J Biomater Sci Polym Ed*, 2014, **25**, 61-74.
43 L. Wang, R. R. Rao and J. P. Stegemann, *Cells Tissues Organs*, 2013, **197**, 333-343.
44 J. Yang, A. Liu, Y. Han, Q. Li, J. Tian and C. Zhou, *J Biomed Mater Res A*, 2014, **102**, 1202-1209.
45 B. Yu, Y. Zhang, X. Li, Q. Wang, Y. Ouyang, Y. Xia, B. Lin, S. Li, Y. Fan and Y. Chen, *J Nanomater*, 2013, Art506593.
46 J. Fan, H. Park, S. Tan and M. Lee, *PLoS ONE*, 2013, **8**, e72474.
47 H. Liu, H. Peng, Y. Wu, C. Zhang, Y. Cai, G. Xu, Q. Li, X. Chen, J. Ji, Y. Zhang and H. W. OuYang, *Biomaterials*, 2013, 34, 4404-4417.
48 W. Chen, H. Zhou, M. D. Weir, M. Tang, C. Bao and H. H. K. Xu, *Tissue Eng Part A*, 2013, **19**, 915-927.
49 S. Ge, N. Zhao, L. Wang, M. Yu, H. Liu, A. Song, J. Huang, G. Wang and P. Yang, *Int J Nanomed*, 2012, **7**, 5405-5414.
50 Y. L. Chen, H. C. Chen, H. Y. Chan, C. K. Chuang, Y. H. Chang and Y. C. Hu, *Biotechnol Bioeng*, 2008, **101**, 821-830.
51 Y. L. Chen, H. P. Lee, H. Y. Chan, L. Y. Sung, H. C. Chen and Y. C. Hu, *Biomaterials*, 2007, **28**, 2294-2305.
52 F. Chicatun, C. E. Pedraza, N. Muja, C. E. Ghezzi, M. D. McKee and S. N. Nazhat, *Tissue Eng Part A*, 2013, **19**, 2553-2564.
53 Z. Schwartz, D. J. Griffon, L. P. Fredericks, H. B. Lee and H. Y. Weng, *Am J Vet Res*, 2011, **72**, 42-50.
54 C. R. Correia, L. S. Moreira-Teixeira, L. Moroni, R. L. Reis, C. A. van Blitterswijk, M. Karperien and J. F. Mano, *Tissue Eng Part C*, 2011, **17**, 717-730.